

## Enhanced antibacterial activity of selenium nanoparticles prepared by cold plasma in liquid

A. A. R. Niema<sup>a,\*</sup>, E. M. Abbas<sup>b</sup>, N. Kh. Abdalameer<sup>c</sup>

<sup>a</sup>*Dept. of Remote sensing and Geographic information systems, College of Science, University of Baghdad*

<sup>b</sup>*Dijlah University College*

<sup>c</sup>*Dept. of Physics, College of Science for Women, University of Baghdad*

In this study, selenium Nanoparticles were synthesized using selenium nitrate in a physical way (using cold plasma produced under normal atmospheric pressure) operating on alternating current AC with a voltage of (13) kV. Its frequency is (23) kHz, and the speed of the Argon gas flow is (3) L/min with an exposure time of 3 min. Selenium Nanoparticles were prepared in four different concentrations (0.2, 0.4, 0.6, and 0.8 ) mM, then the selenium Nanoparticles were characterized by UV-VIS spectroscopy, where (absorption, transmittance, absorption coefficient, energy gap) were measured for all concentrations where it was observed The absorbance increased with the increase in the concentration of the material, while the permeability decreased. The energy gap was at the lowest concentration, 1.74 electron volts. With the increase in concentration, it was noticed that the energy gap decreases, and this is due to the transformation of the material to the nanoscale. Nanoparticle characteristics have been investigated (XRD, AFM, FE-SEM, and UV-Vis). The biological activity of selenium Nanoparticles was tested by the method of diffusion in the medium towards Gram-positive bacteria *Klebsiella Pneumoniae* and Gram-negative *Staphylococcus. aureus*, where the highest inhibition rate was recorded for Gram-negative bacteria, reaching (31, 30, 20, 22) mm, respectively, in the case of bacteria. The positive amount reached (29, 24, 24 20) mm, respectively, where it was noticed that the concentration of the substance increased, the rate of the inhibition diameter increased.

(Received August 16, 2021; Accepted November 19, 2021)

*Keywords:* Plasma in liquid, Selenium, Gram-positive, Gram-negative

### 1. Introduction

Studies have shown that there are several impacts on their features and changes in their characteristics, in nanoscale composite preparation. Many positive effects can be seen on their properties and characteristics. A reinforced mixture (fibers, particles) is a nanocomposite material [1, 2]. Plasma is a collectively behaving quasi neutral gas containing charged and neutral particles. Motions that are dependent not just on local conditions but also on the state of the plasma in distant locations are referred to as collective behavior. Plasma does not adhere to external stimuli because of its collective behavior; rather, it acts as if it had its own mind [3]. The plasma is "quasi neutral," meaning it is neutral enough to take  $n_i \approx n_e \approx n$  ,, where ( $n$ ) is the plasma density ( $n_i$ ) is the ion density, and ( $n_e$ ) is the electron density, but not so neutral that all the relevant electromagnetic forces vanish [4]. Empirical studies have shown that bacterial infections are the most common cause of chronic wounds and mortality. Bacterial infections cause both infections and wounds. Empirical data shows in clinical practice that the antibiotics presently employed mostly kill bacteria by disrupting cell wall production, translation or DNA duplication machinery [5]. Bacteria may become resilient to antibiotics by manufacturing novel enzymes, which are used to de-compose medications and enhance the production of efflux pumps. Resistance [6]. Resistant bacteria have developed rapidly because of the overuse of antibiotics. Pan drug-resistant microorganisms' resistant to all antibiotics have previously been discovered. A potential

worldwide public health concern is now arising from the germs that are multi-drug resistant [7]. As a result, new antibacterial methods are required to combat the increasing issue of these so-called "superbugs" that exhibit pan-drug resistance. While antibiotic resistance mechanisms tend to have little impact on nanoparticles, scientists believe NPs may be used to fight antibiotic-resistant bacteria, since almost all of the resistance mechanisms are completely ineffective. Ag NPs, Au NPs, Se NPs, Pd NPs, TiO<sub>2</sub> NPs, CuO NPs, all antibacterial were shortly to be utilized purposes [8]. Se NPs have garnered growing interest, with a variety of studies demonstrating the potential for antimicrobial activity, particularly in regard to bacteria and fungus, as well as the capacity to break biofilms [9]. Selenium, as opposed to gold, silver, platinum and titanium, is a human body trace element. It is a cofactor for glutathione peroxidases and thioredoxin reductases and is required in at least 25 selenoenzymes [10]. Research at the present time is investigating the function of Se nanoparticles manufactured by biotechnological means on the eradication of e. Growth of coliform bacteria and Staphylococcus, along with its explanation of the growth control mechanism, can serve to reveal the growth-limiting mechanism. The tests XRD, UV, and SEM, TEM, and AFM were employed to analyze these materials.

### 1.1. Plasma generation in liquid

Various experimental settings have been described for plasma production in liquid, including the characteristics of the liquid medium, electrode material, electrode arrangement, and electricity source [11]. Plasma in liquid production may be split into four major categories based on electrode designs and power sources [12]:

- (i) An electrochemical gas discharge.
- (ii) Direct electrode discharge.
- (iii) In this case, an electrode touches the electrolyte, resulting in contact discharge.
- (iv) The production of RF and MW.

## 2. Materials and methods

Plasma Jet at Atmospheric Pressure in Liquid Technique. The experimental configuration utilized to synthesize colloidal nanoparticles is illustrated in figure (1).

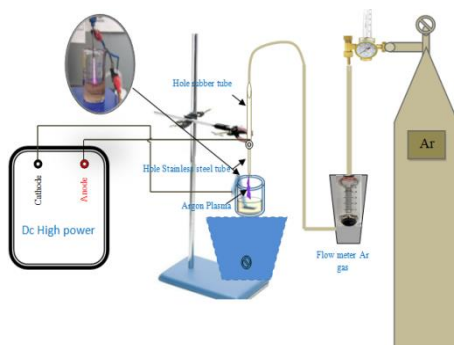


Fig.1. Scheme of plasma jet system (cold plasma).

### 2.1. Materials

(i) Nitrate, Selenium (SeO(NO<sub>3</sub>)<sub>2</sub>), molecular Weight: 218.96 g/mol, Color: Reddish, easy to dissolve in cold water. Is used as metallic precursor for preparation Se NPs.

(ii) Fructose (C<sub>6</sub>H<sub>12</sub>O<sub>6</sub>), molecular Weight: 180.16 g/mole, Color: white, easily soluble in cold water. Is used as a stabilizing agent to prevent Nanoparticles from aggregation.

### 2.3. Preparation of SeO(NO<sub>3</sub>)<sub>2</sub> aqueous solution

An aqueous solution of selenium nitrate is prepared differently Concentrations, (0.0218, 0.0437, 0.0656, 0.0875) grams of de- ionized SeO(NO<sub>3</sub>)<sub>2</sub> to 500 ml water (DI) to concentrations of

(0.2, 0.4, 0.6, 0.8) mM respectively then Move carefully with a stirrer to get the fructose solution homogeneous The aqueous solution is used as a stabilizing agent to prevent Se NPs from Aggregation, to prepare 0.01 M fructose (0.04) g of it to 25 ml DI is added, also stirred by a motor to obtain homogeneity. Then mixed with a solution of  $\text{SeO}(\text{NO}_3)_2$ .

#### 2.4. Synthesis Se Nanoparticles Colloidal

The Se NP's Synthesis involves the use of a high tension of about 13 kV, and then the plasma forms between the capillaries and the  $\text{SeO}(\text{NO}_3)_2$  aqueous solution. The high-energy and ionic charged electrons (Ar), which are present in plasma, begin to flow in the circuit and current (about a few thousand amperes). A few minutes after the discharge begins, the solutions become reddish-orange as indicated in the figure.2 a sign of Se NPs production. The exposure duration for each concentration was found to be 3 minutes. The colored solution was then marked using a measuring tool.

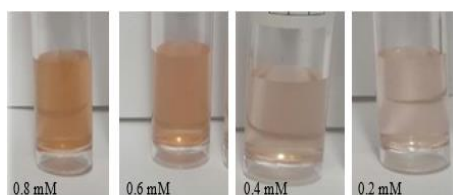


Fig. 2. Colored Se NP solutions according to different plasma treatment concentrations at 3 minutes.

### 3. Results and discussion

#### 3.1. Se Nanoparticles Structure Identification

XRD measurement of selenium nanoparticles requires determining the structure of Se nanoparticles. Different amounts of selenium (0.2, 0.4, 0.6 and 0.8) mM were used to make the particles. After depositing the particles on glass bases using the drop coating method, the maximum concentration (0.8 mM) was used to measure the structure and size of the particles. The XRD diffraction peaks (Fig. 3) are indexed with the hexagonal Se lattice levels (100), (101), (110), (102), (111), 200), (201), and (003), and are in good agreement with the vertices marked in Standard Card (PDF 65-1876) [13]. The Se nanoparticles formed in a pure trigonal phase, according to the XRD pattern shown above. This XRD pattern yielded network constants of  $a = 0.436$  nm,  $b = 0.496$  nm, which are compatible with those published in the literature ( $a = 0.436$  nm,  $b = 0.495$  nm) [14].

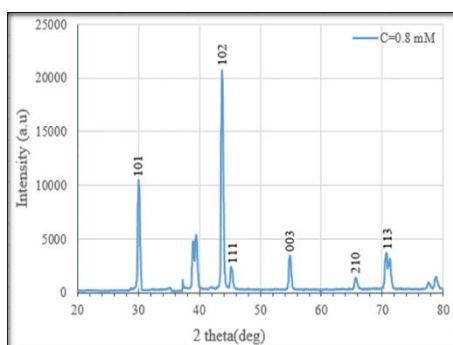


Fig. 3. XRD diffraction pattern of Se thin film deposited on glass substrate.

#### Optical Energy Band Gap ( $E_g$ ) of the Selenium Nanoparticles

Absorption coefficient ( $\alpha$ ) associated with the strong absorption region of the sample was calculated from absorbent ( $A$ ) and the sample thickness ( $t$ ) by using the relation [15]:

$$\alpha = 2.303 A/t \quad (1)$$

The direct optical band gap for SeNPs obtained under optimal conditions was calculated from the optical absorption spectra by using the Tauc relation in equation [16,17]:

$$(\alpha h\nu) = A(h\nu - E_g)^r \quad (2)$$

When calculating the energy gap, it was found that its value ranged between (1.46-1.71) eV, and a decrease in the energy gap values was observed as the concentration of the substance increased as shown in Figure (4) and Table (1). energy and near the conduction beam and thus the absorption of photons with low energy increases, and this agrees with the results of [10].

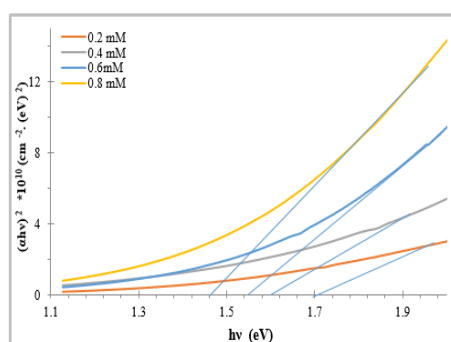


Fig. 4. Variation of  $(\alpha h\nu)^2$  with  $h\nu$  for Se NPs for four concentrations (0.2, 0.4, 0.6, and 0.8) mM and time exposure 3 min.

Table 1. Optical Energy Band Gap ( $E_g$ ) of the Se NPs from UV-Vis absorption spectra.

Concentration Se NPs mM	Optical Band gap $E_g$ (eV)
0.2	1.71
0.4	1.605
0.6	1.55
0.8	1.46

### 3.2. Se Nanoparticles Micro structure

FE-SEM was used to analyze the particle size of selenium Nanoparticles and the results are shown in Fig. 5A. The size distribution of Se NPs in the sample was revealed by microscopic imaging; the discovered Se NPs were spherical in shape (Fig. 5b). SEM micrographs of selenium Nanoparticles revealed a size distribution of 500–600 nm, which is highly narrow (Fig. 5C).

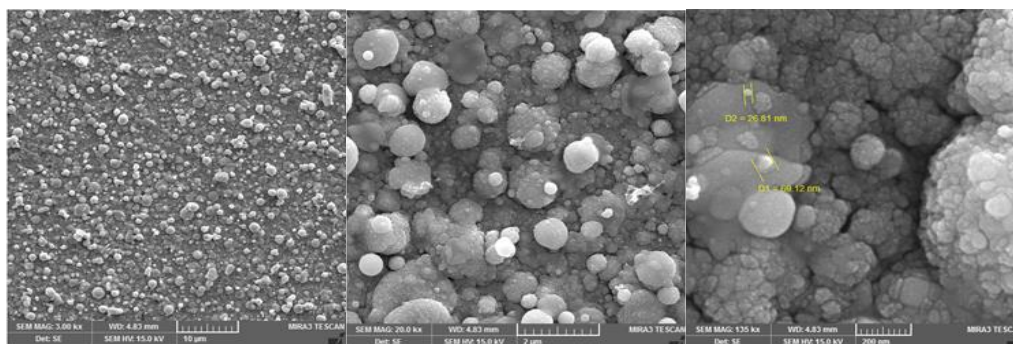


Fig. 5. FE-SEM images of Se Nanoparticles measurement at range (200nm, 2µm and 10 µm) with concentration (0.8) mM.

### 3.3. Se Nanoparticles Morphological analysis

AFM technique was employed in this study to investigate the effect of surface roughness of material (Se) on the characteristic of inhibition of bacteria with different concentration (0.2, 0.4, 0.6 and 0.8) mM; Fig. 6 shows the mode AFM images of the Se which was deposited on glass. Fig. 6 (0.8 mM) shows a soft surface with very good adhesion, and has grain size about 76.82 nm.

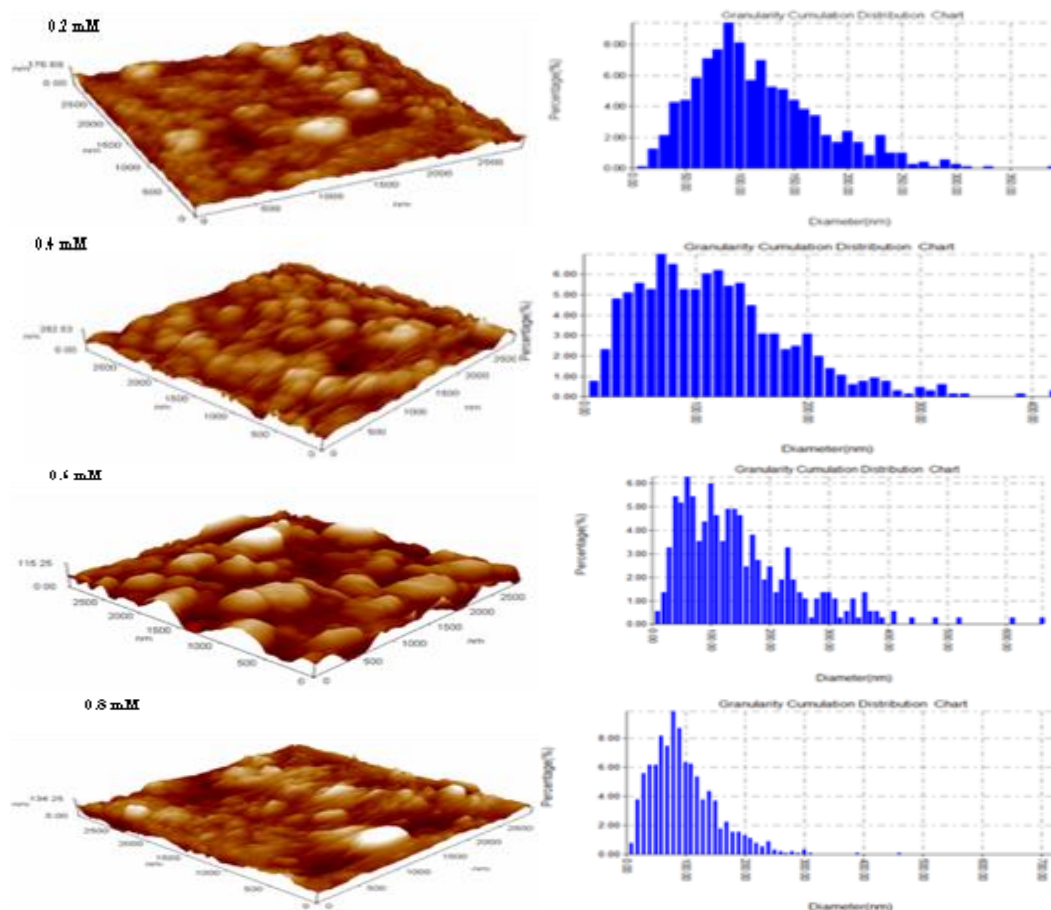


Fig. 6. 3D AFM micrographs of Se NPs deposited on glass substrate with different concentration (0.2, 0.4, 0.6 and 0.8) mM.

Table 2. AFM parameters of the Se NPs deposited with different concentration (0.2, 0.4, 0.6 and 0.8) mM.

Se Nanoparticles			
Concentration mM	Avg. Diameter (nm)	Root Mean Sq. (nm)	Ave. Roughness (nm)
0.2	54.45	9.11	7.65
0.4	62.76	11.6	8.32
0.6	67.8	15.3	10.54
0.8	76.823	17.3	14.32

### 3.4. Antibacterial Activity of the Selenium Nanoparticles

The physical synthesis of Se NPs showed excellent antibacterial activity Clinically isolated, multidrug-resistant human pathogens such as Gram-positive bacteria i.e., *Staphylococcus aureus* and Gram-negative bacteria i.e., *Klebsiella pneumonia* and at different concentrations as shown in Figure (7). The inhibitory area diameter, measured and tabulated in Table (3) in this experiment. Selected pathogenic bacteria and yeasts was achieved in triplicates and the obtained results were statistically analyzed. The means and standard deviation (means  $\pm$  SD) were calculated and reported for all treatments and compared with control. The significant levels were considered at  $p < 0.0001$  using t-test as shown in Figure (8). The result showed the *Staphylococcus aureus* bacteria occupied larger zones of inhibition, than bacteria compared with the *Klebsiella pneumoniae*, which may be due to the variation in cell wall composition<sup>13</sup>. The physical synthesized Se nanoparticles by using cold plasma also showed a similar potent antibacterial activity [19].



Fig. 7. Activity of Se NPs against bacteria with clear zones of inhibition with various concentrations of Se NPs for (0.2, 0.4, 0.6, and 0.8) mM and time exposure 3 min.

Table 3. Results of the antibacterial activity of biologically synthesized of Se NPs by cold plasma.

Name of the Microorganisms	Diameter of inhibition zone (mm)							
	0.2 mM		0.4 mM		0.6 mM		0.8 mM	
	Mean	SD	Mean	SD	Mean	SD	Mean	SD
<i>Staphylococcus aureus</i>	20	$\pm 0.35$	22	$\pm 0.35$	30	$\pm 0.70$	31	$\pm 0.31$
<i>Klebsiella pneumoniae</i>	20	$\pm 0.63$	24	$\pm 0.35$	24	$\pm 0.33$	29	$\pm 0.31$

\*Values expressed as mean  $\pm$  SD

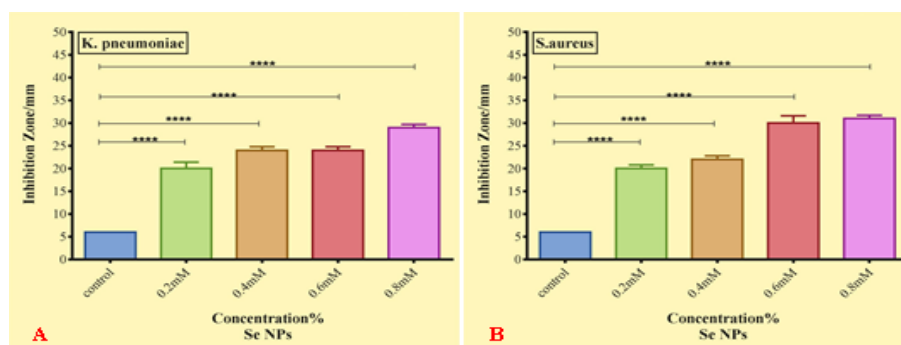


Fig. 8. Effect Se NPs prepared in four different concentrations (0.2, 0.4, 0.6, and 0.8) mM against some clinical isolates of bacteria and yeasts, A: *k. pneumoniae*, B: *S. aureus*, the effect was measured by the inhibition zone formed around wells filed by Se NPs, statistical analysis reported as the means values followed by the letters are significantly, \* $p < 0.05$ , \*\* $p < 0.01$ , \*\*\* $p < 0.001$ , \*\*\*\* $p < 0.0001$  (\*) compared with control group. Errors bars represent SD of Triplicate experiments.

#### 4. Conclusion

Experimental evidence indicates that our approach outperforms the other competing methods and may be used to a wide range of biomedical and nanotechnology applications, as shown in this research. The mean size of Se NPs rises with concentration. The produced Se-NPs have a spherical form and are almost Gaussian. X-ray diffraction for nanoparticles generated shows that the samples have little crystalline size, the resultant SEM picture shows nanoparticles that range from too little.

#### References

- [1] M. Hasanpour, M. Niyafar, J. Amighian, Journal of magnetism and magnetic materials 334, (2013).
- [2] Mazhir, S. N., Ali, A. H., Abdalameer, N. K. & Hadi, F. W. in International Conference on Signal Processing, Communication, Power and Embedded System, SCOPES 2016 - Proceedings (2017)
- [3] S. N. Mazhir, ARPN Journal of Engineering and Applied Sciences 13(3), 864 (2018).
- [4] A. Q. Muryoush, A. H. Ali, H. Al-Ahmed Iraqi Journal of Science 60(9), 1997 (2019).
- [5] M. Vahdati, T. T. Moghadam, Sci. Rep. 10(510), 1 (2020).
- [6] T. Huang, S. Kumari, H. Herold, T. B. Aigner, Int. J. Nanomedicine 15, 4275 (2020).
- [7] L. D. Geoffrion, T. Hesabizadeh, D. Medina-Crus, ACS Omega. 5(6), 2660 (2020).
- [8] N. Filipović, D. Usjak, M. T. Milenkovic, K. Zheng, Front. Bioeng. Biotechnol. 8, 624621 (2021).
- [9] T. H. D. Nguyen, B. Vardhanabhuti, M. Lin, A. Mustapha, Food Control. 77, 17 (2017).
- [10] F. Jiang, W. Cai, G. Tan, Nanoscale Res. Lett. 12, 0 (2017).
- [11] G. Saito, T. Akiyama, J. Nanomater. 2015, (2015).
- [12] R. A. Hammoodi, A. K. Abbas, M. K. Khalaf, Indian Journal of Natural Sciences 9(53), 17257 (2019).
- [13] D. Velauthapillai, R. Rajamani, C. S. Bellan, K. Arts, Int. J. Biosci. Nanosci. 2(4), 78 (2015).
- [14] Z. Chen, Y. Shen, A. Xie, J. Zhu, Z. Wu, Cryst. Growth Des. 9(3), 1327 (2009).
- [15] C. I. Nweze, A. J. Ekpunobi, African Rev. Phys. 10, 105 (2015).
- [16] A. S. Hassanien, K. A. Aly, A. A. Akl, J. Alloys Compd. 685, 733 (2016).
- [17] K. A. Aadim, S. N. Mazhir, N. Kh. Abdalameer, A. H. Ali, IOP. Conf. Ser.: Mater. Sci. Eng. 987, 012020 (2020).
- [18] K. Nithya, S. Kalyanasundharam, OpenNano 4, 2 (2019).
- [19] H. Yang, Y. Ren, T. Wang, C. Wang, Results Phys. 6, 299 (2016).